Object Tracking in Random Access Networks: A Large Scale Design

Mohammadreza Alimadadi, Milica Stojanovic, *Fellow, IEEE,* and Pau Closas, *Senior Member, IEEE*

Abstract—We address a scenario in which networked sensor nodes measure the strength of the field generated by a number of moving objects and transmit their measurements to a fusion center in a random access manner for final reconstruction of the objects' trajectories. To ensure scalability over an arbitrary coverage area, we divide the total observation area into design units, each consisting of several sensing cells. An extended Kalman filter is assigned to each cell, while neighboring cells communicate with each other to exchange current status, thus allowing state fusion whereby the Kalman filters adjust (over-write) their local estimates at the end of each updating interval. In this manner, provisions are made for the objects leaving and entering a design unit, yielding a system design that is scalable across a large coverage area without an increase in complexity (size) of the Kalman filters. We provide a step-by-step procedure for designing the system, taking into account the fact that sensors communicate to the fusion centers using random access over band-limited and imperfect channels where packet loss is inevitable due to collisions as well as communication noise. In addition, we study different rate control schemes in which the fusion center instructs the sensors to increase or decrease their sensing (transmission) rate in accordance with the currently estimated object locations. Performance is evaluated through simulation, showing the effectiveness of the approach proposed in terms of the mean squared localization error and data throughput, and quantifying the effect of limited bandwidth and lossy communication.

Index Terms—Kalman filter, object tracking, wireless sensor network, adaptive rate control, random access, large coverage, underwater acoustic communications.

I. INTRODUCTION

A Wireless sensor network (WSN) is an ad-hoc network composed of resource-constrained devices called sensor nodes. The sensors are able to perceive the environment, collect, process, and exchange data. A WSN may be designed with different objectives in mind, such as event monitoring, data gathering, agent actuation, and object tracking [1], [2]. With increased human activity in the oceans, underwater acoustic sensor networks (UASNs) have recently drawn research attention as a promising technology to monitor and explore the oceans [3]. These networks rely on acoustic transmission for spanning longer ranges, and are consequently constrained by limited bandwidth, long propagation delays and pronounced Doppler effects. The data gathering of UASNs is still severely limited because of the acoustic channel communication characteristics [4]–[6]. Random access relieves syn-

chronization issues in such conditions, but introduces the risk of data packet collision at the fusion center (FC) of a network. To manage the scarce bandwidth and power resources, efficient control schemes are often necessary in UASNs [7].

One of the important applications of WSNs is object tracking, which has been studied extensively for several decades and numerous tracking algorithms have been proposed [8], [9]. However, object tracking still remains a very challenging problem [10]. Tracking algorithms aim at maintaining accuracy and reporting the results quickly, while reducing communication costs and energy consumption [11]–[15]. In [16], a decentralized, dynamic clustering algorithm was introduced for acoustic object tracking. The authors in [17] considered the joint problem of packet scheduling and self-localization in underwater acoustic sensor networks and proposed a Gauss-Newton based localization algorithm for these schemes. In order to manage the resource scarcity of UASNs, [18] introduced an adaptive object tracking approach where sensor nodes transmit to the FC using random access in a centralized topology.

Kalman filtering is by far the most popular method for object tracking. In [19], the authors considered the case where the packets may be lost due to collisions and communication noise, which is known in the literature as Kalman filtering with intermittent observations (KFIO). The authors in [20] studied the stability of standard KFIO. They showed the existence of a critical arrival rate below which the estimator may diverge.

Inspired by these studies, several authors have studied different aspects of KFIO, using different network models and protocols [21]–[23]. In [24], authors extended the existing results to a more general setting in which the measurement equation, i.e., the measurement matrix and the measurement error covariance, are random. For this setting, necessary and sufficient conditions for stability were stated and assessed numerically. The result generalizes the existing ones in the sense that it does not require the system matrix to be diagonalizable.

In [25], Kalman-filtered compressed sensing was studied and its performance quantified in the presence of measurement losses. Using input-to-state stability analysis, the authors provided an upper bound on the covariance of the estimation error for a given rate of information loss. The authors in [26] considered distributed nonlinear state estimation over WSNs where data exchanges occur only among the neighborhoods of sensors. They obtained a nonlinear KFIO based on cubature Kalman filter [27]. An equivalent information filter was subsequently derived, and the diffusion cubature KFIO was designed based on this filter.

In this paper, we propose a scalable approach for designing random access sensor networks for object tracking in a large

area, where extended Kalman filtering (EKF) is employed as the estimation method. Similarly to [28], we assume that the sensor nodes access the channel in a random manner. As a result, the packets may be lost due to collisions or communication noise. To ensure geographical scalability, we divide the observation area into design units and sensing cells whose Kalman filters exchange information to enable state fusion which in turn ensures tracking of objects as they cross unit boundaries. We refer to this approach as zoning. We propose two fusion methods that efficiently combine the Kalman filter estimates, namely soft fusion with overwriting and hybrid fusion. We outline a procedure for determining different system parameters that ensure a desired performance subject to the limited amount of bandwidth available. In addition, we study different rate control schemes as a way to improve the system performance within the communication constraints. The proposed method is scalable and easily extends to an arbitrary coverage area without the need to change the structure of the network or the Kalman filtering process whose complexity remains determined by the size of the design unit, not the size of the entire area covered. In addition to improving the energy efficiency and computational complexity of the system, our approach reduces the probability of Kalman filter divergence, and addresses the issue of tracking a variable number of objects (objects entering and departing the sensing area of a single FC) without requiring the use of more complex tracking schemes. Simulation results show the benefits of the proposed method.

The main contributions of this paper are as follows:

- We introduce a scalable method for designing a random-access sensor network for object tracking using EKF with intermittent observations (i.e., imperfect communication).
- We introduce two new fusion methods (soft fusion with state overwriting and hybrid fusion) and show their superior performance compared to the soft fusion without overwriting [29].
- We propose methods for adaptive adjustment of transmission rate and optimize the relevant control parameters.

The rest of the paper is organized as follows. Sec. II presents the system model. Sec. III details the design method for object tracking in random access networks. Sec. IV discusses the proposed fusion methods. Simulation results are presented in Sec. V. Finally, we provide concluding remarks in Sec. VI.

II. SYSTEM MODEL

We consider an observation area of arbitrary size in which a number of objects are located. The location and the velocity of the m-th object at time interval k are denoted by

$$\mathbf{x}_k(m) = [x_k(m)\ y_k(m)\ \dot{x}_k(m)\ \dot{y}_k(m)]^\top \quad (1)$$

We assume that the objects are placed across the area uniformly at random with density ρ_o objects/m^2. Each object emits a signal of certain amplitude. The signal decays with distance d based on a signature function $\mathrm{f}(d)$ which is assumed to be known (e.g. exponential decay, distance-squared decay, etc.).

A number of sensor nodes are distributed across the observation area. Each node has a sensor that takes measurements of the field generated by the objects. At time interval k the received signal at the n-th sensor is modeled as

$$v_k(n) = \sum_m \mathrm{f}(d_k(m,n)) + w_k(n) \quad (2)$$

where $d_k(m,n)$ is the distance between the m-th object and the n-th sensor at time k, and $w_k(n)$ is the sensing noise, modeled as zero-mean Gaussian with variance σ_w^2.

After sensing the field, each node encodes its measurement $v_k(n)$ into a digital data packet, adds its ID, and transmits the packet to the FC. The transmissions occur at random instants in time, which we model here as a Poisson process with rate λ [packets/s] per sensor. The Poisson model is used as a general case, but other models could be used as well.

The FC collects the packets transmitted in one time interval of duration T, which is chosen short enough that the objects' locations can be considered fixed over it. Some packets will be dropped because of collisions and noise. After discarding the erroneous packets, the FC is left with useful packets, which arrive at an aggregate rate λ_{FC}. These intermittent observations are then used as an input to the tracking algorithm to estimate the location of the objects.

We define the state of the system at time k as

$$\mathbf{x}_k = [\mathbf{x}_k(1)\ \mathbf{x}_k(2)\ \ldots\ \mathbf{x}_k(M)]^\top \quad (3)$$

where M is the maximum number of objects to be tracked by one FC and $\mathbf{x}_k(m)$ is defined in (1). We assume that the state vector evolves linearly as

$$\mathbf{x}_k = \mathbf{A}\mathbf{x}_{k-1} + \mathbf{q}_k \quad (4)$$

where $\mathbf{A}$ is the state transition matrix, and $\mathbf{q}_k$ is the process noise, which is modeled as zero-mean Gaussian with covariance $\mathbf{Q}$. For example, if we consider an auto-regressive model of order 1 (AR-1) with one-step correlation coefficient ρ and a single object to be tracked, the $\mathbf{A}$ and $\mathbf{Q}$ matrices become

$$\mathbf{A} = \begin{bmatrix} 1 & 0 & T & 0 \\ 0 & 1 & 0 & T \\ 0 & 0 & \rho & 0 \\ 0 & 0 & 0 & \rho \end{bmatrix}, \quad \mathbf{Q} = \begin{bmatrix} 0 & 0 & 0 & 0 \\ 0 & 0 & 0 & 0 \\ 0 & 0 & 1 & 0 \\ 0 & 0 & 0 & 1 \end{bmatrix} \sigma_v^2(1-\rho^2)$$

where σ_v^2 represents the variance of object's velocity, i.e. the system uncertainty. The AR-1 model is used here only as an example. Our treatment is not limited to it and applies to other models as well.

It may be worth noting at this point the three degrees of randomness that govern the system behavior: sensing noise that interferes with the measurements, process noise that causes uncertainty in the objects' locations, and communication noise that causes packet loss. The three processes act independently, but each has an adverse effect on the quality of tracking.

Different methods can be used to estimate the location of objects using intermittent observations, including gradient descent or sparse recovery. The modified lossy extended Kalman filter (MLEKF) was proposed in [19] as a method for incorporating intermittent observations into the EKF. In this paper we use the MLEKF as the estimation method for

the locations of objects. Essentially, a MLEKF is an EKF whose measurement matrix is changing randomly based on the random set of nodes that contribute measurements in each updating interval. For details of MLEKF implementation, the reader is referred to [19].

Our goal is to design the random-access sensor network so as to satisfy certain criteria such as specific tracking accuracy or data throughput, given the limited amount of resources available. The design process includes choosing the size of sensing units, the density of sensors, the length of the collection interval and the sensors' transmission rate. The network design should be scalable so that one can easily add new areas if the need arises, ensuring arbitrary coverage at only a linear increase in transmission power and manageable complexity.

III. SCALABLE DESIGN FOR LARGE COVERAGE

Tracking methods described in the referenced literature are designed based on the assumption that the observation area is fixed and the number of objects in the area is known a-priori, so that one can easily define the state vector and employ Bayesian filtering for location estimation. These assumptions are not realistic in localization and tracking applications where large coverage is needed and objects can freely enter or depart a local area. Power consumption and computational complexity are two additional factors that must be considered when scalability to a large coverage area is needed and having a single FC is not a desirable option.

A. Zoning: Design units, sensing cells, and the isolation rule

To make the design process as systematic and scalable as possible we introduce the concept of zoning in which a *design unit* (DU) acts as the smallest unit for the design process. Each DU consists of a number of *sensing cells*. The design process applied to one DU is repeated across an arbitrary coverage area. Fig. 1 illustrates the concept.

We consider hexagonal cells as a good approximation for spherical signal spreading, but other approximations are possible as well. Assigned to each cell is an FC whose task is to report on the objects found in the entire DU. To do so, the FC conducts a two-step procedure: (1) it collects data packets from the sensors located within its cell (an occasional packet from a neighboring cell does not interfere with the process and can be accepted as well), and (2) it exchanges information with the FCs within its DU (six surrounding cells) at the end of each collection interval. The exchange of information between the neighboring FCs occurs over a separate infrastructure, which does not share the same communication bandwidth with the sensors. In underwater acoustic scenarios, for instance, the FCs can be connected by radio links (if close to shore) or by satellite links (if remote).

The sensors within the central cell pick up the signals from objects within the entire DU, not only within the cell itself. The radius R_c of the cell, however, is designed such that the objects outside of the DU are not picked up by the sensors located within the central cell. We call this principle the isolation rule. The Kalman filter running at each FC is thus set to handle a maximum number of objects expected in one DU (a number that can be chosen based on historical data pertaining to the specific application).

In exchanging the information with its neighboring FCs, the neighbors act as helpers, as the information they have about the objects located within their cells is likely more accurate. The design process applied to one DU is replicated at every other unit, as each cell acts both as the center of its DU and an outer member of six other DUs (a helper to six other central cells). Expansion of the coverage area thus entails only a linear increase in the number of FCs. The total power used for communication follows the same trend, while the computational complexity of Kalman filtering and data fusion remains determined by the number of objects within a single DU.

B. System parameters

Table I shows the parameters involved in the design process. Some parameters, such as the object and the node density, are initially defined, and we will define the rest gradually as we consider their impact on the overall system performance.

1) Cell radius: To determine the cell radius, let us consider the case where an object emits a signal of power P_t and the signal amplitude decays based on an exponential

TABLE I: Parameters involved in the design process

| Parameter	Description
ρ_o	object density [objects/m^2]
ρ_s	node density [nodes/m^2]
B	bandwidth [Hz]
f(d)	signature function (path loss model)
T	collection interval [s]
L_p	packet length [bits]
T_p	packet duration [s]
R_c	cell radius [m]
N	number of nodes in a cell
M	maximum number of objects in a DU
SNR_c	minimum SNR needed for sensing
ρ	AR-1 correlation factor
σ_v	AR-1 standard deviation of the object's speed [m/s]
p_e	probability of packet being lost to communication noise
σ_w	standard deviation of the sensing noise
P_t	transmission power [W]
$\lambda(n)$	transmission rate of the n-th sensor [packets/s]
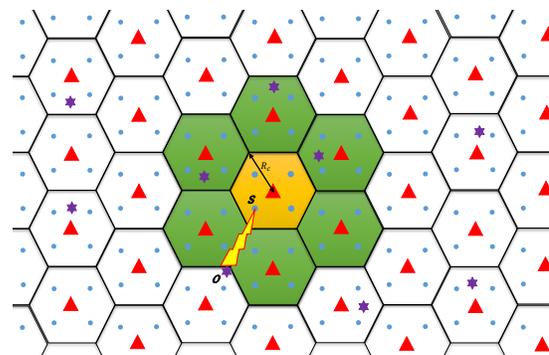
Fig. 1: The entire area is divided into sensing cells, and a fusion center is assigned to each cell. Sensor nodes are shown as circles, fusion centers as triangles, and moving objects as stars. A central cell and six surrounding cells form a design unit (DU). The radius R_c of a cell is chosen such that the sensors located in the central cell pick up the signals of the objects located within the DU but not outside of it. The design process applied to one DU is repeated across the entire area.

signature function $f(d) = e^{-\alpha d}$ where α is the decay rate and d the distance. Denoting by SNR_c the sensing signal to noise ratio (SNR) below which an object is not sensed by a node (an "SNR curtain"), the isolation rule dictates that $P_t f^2(R_c)/\sigma_w^2 \le SNR_c$. The cell radius is thus found from the condition $R_c \ge R_{min}$, where $R_{min} = \frac{1}{2\alpha} \ln \frac{P_t/\sigma_w^2}{SNR_c}$ for the exponential signature, or an appropriately determined value for a different type of signature.

While zoning ensures scalability to arbitrary coverage areas, it is interesting to note that it also supports frequency reuse, which is critical for applications in underwater acoustic scenarios where the bandwidth is limited.

2) Collection interval T: The Kalman filter running at each FC is updated at the end of every collection interval T. During this interval of time, the sensors presumably see a static placement of objects, i.e. T should be chosen short enough that any movement of objects is negligible from the viewpoint of localization.

Denoting by d_X the desired spatial resolution that can be achieved for a given signature function, and noting that the average expected speed is proportional to σ_v ($\sqrt{\frac{2}{\pi}}\sigma_v$ for the AR-1 model), we have that $T < d_X/\sigma_v$. For example, if we define d_X as the distance at which the object's strength delays by X dB, for the exponential signature we have that $d_X = \frac{\ln 10}{2\alpha}X$; hence, $T < 1/\alpha\sigma_v$ is an appropriate choice.

3) Number of nodes per cell and transmission rate: Each packet consists of a header and a payload. The header is the identity of the sensor from which the packet originated. The payload carries the sensed value. Denoting by $\bar{L}_p$ the payload size and by N the number of sensors in a sensing cell, the length of a packet is

$$L_p = \bar{L}_p + \lceil \log_2(N) \rceil \qquad (5)$$

As we mentioned earlier, nodes transmit packets based on a Poisson process with rate λ per sensor and the FC collects the packets during an interval T. Following the treatment of [28], the rate of useful packets at the FC is modeled as a Poisson process with aggregate arrival rate

$$\lambda_{FC} = \frac{N}{T}\left(1 - e^{-p\lambda T}\right) \qquad (6)$$

where $p = (1 - p_e)e^{-2N\lambda T_p}$, p_e is the probability of a packet being lost to communication noise and T_p is the packet duration. The optimal per node transmission rate which maximizes λ_{FC} can then be shown to be

$$\lambda_{opt} = (2NT_p)^{-1} \ [\text{packets/s}] \qquad (7)$$

Using this value in (6), we find the corresponding aggregate rate of useful packets at the FC as

$$\lambda_{FC,max} = \frac{N}{T}\left(1 - e^{-\frac{(1-p_e)T}{2NT_p e}}\right) \qquad (8)$$

which is the maximum achievable rate at which the FC can receive packets from sensor nodes transmitting at a fixed rate.

Substituting for the packet duration as $T_p = L_p/B$, where B is the system bandwidth, the aggregate throughput $\lambda_{FC,max}$ is obtained as a function of N,

$$\lambda_{FC,max} = \frac{N}{T}\left(1 - e^{-\frac{(1-p_e)TB}{2Ne(\bar{L}_p + \lceil \log_2(N) \rceil)}}\right) \qquad (9)$$

The optimal number of nodes per cell that maximizes $\lambda_{FC,max}$ cannot be obtained in closed form, but it can be evaluated numerically for a given set of $\bar{L}_p$, B, p_e and T. Fig. 2 shows the result for a variety of network parameters. Given the system bandwidth B, this result points to the value N_{opt}, which in turn yields the transmission rate (7) as well as the sensor density ρ_s. In case the resulting ρ_s is unacceptably high, one can always use fewer nodes per cell, with the understanding that the data throughut will be sub-optimal. Algorithm 1 summarizes the steps for designing the system.

C. Adaptive rate control

The fixed rate control scheme discussed above is a simple method for setting the sensors' transmission rate. As the packets from different sensors may have different importance, adaptive rate control can potentially improve the tracking accuracy and the bandwidth efficiency of the system. In [30] several rate control schemes were proposed, and we briefly review them here.

a) Exponential rate control: This scheme distributes transmission rate exponentially according to the distance to the nearest object. Denoting by $d_k(n)$ the distance from sensor n to the closest object it sees at time k, the transmission rate assigned to the n-th sensor at time k is

$$\lambda_k(n) = \lambda_k^e e^{-\frac{d_k^2(n)}{\sigma_e^2}} \qquad (10)$$

where λ_k^e and σ_e are control parameters. While σ_e controls the transmission priority radius around the object, λ_k^e can be determined from the optimality condition (7) such that the total transmission rate satisfies $\sum_{n=1}^{N} \lambda_k(n) = (2T_p)^{-1}$, i.e.

$$\lambda_k^e = \frac{1}{2T_p \sum_{n=1}^{N} e^{-\frac{d_k^2(n)}{\sigma_e^2}}} \qquad (11)$$

which specifies the rate control scheme in (10).

b) Relative power rate control scheme: This scheme is based on the intuition that the sensors which receive a more powerful signal in a given collection interval should have higher transmission rate in that interval. Based on this method, at time k the n-th sensor transmits at rate
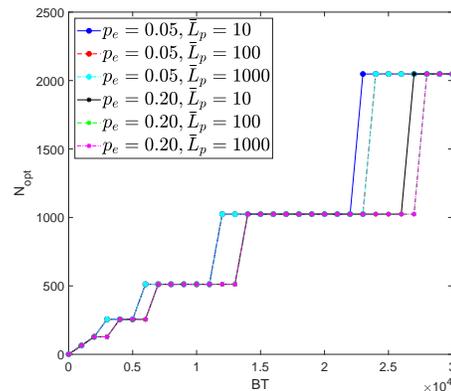

Fig. 2: Optimal number of nodes per cell as a function of bandwidth.

$$\lambda_k(n) = \frac{1}{2T_p} \left(\frac{v_k(n)}{\sum_{i=1}^{N} v_k(i)} \right) \tag{12}$$

While we are focusing here on the received signal strength as a source of information for the objects' location, other factors such as time of arrival could be considered as well.

Rate control is particularly advantageous in situations where there is not enough bandwidth available. By assigning more transmission opportunities to the nodes that carry more useful information, the available bandwidth is used more efficiently.

IV. DATA FUSION

At the end of a collection interval, each FC has an estimate of the state vector corresponding to the objects within its DU. We call this local estimate a *partial estimate*. The FCs of one DU exchange their partial estimates in order to reach a consensus on all the objects within a DU. The method used for this purpose is called the fusion method.

Each FC is independently responsible for combining all the partial estimates in an efficient way in order to obtain its final estimate. Since the fusion process executed in each sensing cell is identical, any additional cell will simply replicate it. Tracking in a new cell remains the same. The Kalman filters still operate on the same state dimension M, which corresponds to the maximum number of objects expected in one DU, not the total observation area. Thus, the algorithm implemented at each FC retains the same computational complexity, while the total coverage area can grow without bounds.

Coupled with the design procedure outlined in the previous section, data fusion has a number of other advantages. First, one does not need to be concerned about the objects crossing the cell boundaries, nor about the unknown number of objects inside each sensing cell. As long as the design parameter M covers the objects inside a DU, data fusion will take care of any objects entering or departing a cell. Second, the computational complexity is lower compared to the case where a single Kalman filter covers multiple cells. This is due to the fact that the size of matrices involved in Kalman filtering increases with the number of objects being tracked and the complexity is a non-linear function of the size of the matrices. Moreover, the power consumption is lower with zoning as now each sensor needs only to reach the nearest FC and not the single global FC.

Below, we review two existing fusion methods and introduce two new ones.

Algorithm 1 Network design process

Input: B, p_e, $\bar{L}_p$, $f(d)$, SNR_c, σ_v
  1: Determine R_{min} based on the path loss model (object signature function) and the isolation rule. Set the cell radius to $R_c = R_{min}$
  2: Choose T based on the speed of objects and the path loss model $T < \frac{d_X}{\sigma_v}$
  3: Find N_{opt} that maximizes (9). Set $N = N_{opt}$
  4: Find λ_{opt} from and (7). Set $\lambda = \lambda_{opt}$
Output: R_c, T, N and λ

---

1) State overlapping (hard-fusion with overwriting): In [30] a fusion method called state overlapping was proposed, which is based on exchanging and overwriting the estimated state vectors between a number of independent Kalman filters. At the end of each collection interval the estimated locations of objects (partial estimates) are checked. If an object is estimated to be in the i-th cell, the corresponding state in all other Kalman filters will be overwritten by the estimated value of the i-th filter. Such an approach is justified by the fact that whenever an object is inside the i-th cell, the estimate obtained by the i-th Kalman filter is expected to be more reliable than the ones obtained by other filters. Consequently, we simply discard the less reliable values and continue with the more reliable one.

In practice, the Kalman filter needs to be updated only in those cells in which an object is found at time k. This further reduces the computational complexity and is an appealing feature of the state overlapping method.

2) Linear soft-fusion: Instead of overwriting, linear soft-fusion can be used, where the final estimate is formed as a weighted average of all partial estimates. Optimally, the weights come from the covariance matrix of the estimates so that a more reliable estimator has a larger weight than a less reliable one [29]. In linear soft-fusion, the final estimate is given by

$$\widehat{\mathbf{x}}_k = \sum_{l=1}^{L} \mathbf{\Xi}_k^l \widehat{\mathbf{x}}_k^l \tag{13}$$

where $\widehat{\mathbf{x}}_k^l$ is the estimated state vector of the l-th FC at time k and $\mathbf{\Xi}_k^l, l = 1, \dots, L$ are $D \times D$ weighting matrices, where L is the number of FCs in a DU (for hexagonal cells $L = 7$) and $D = 4M$ is the size of the state vector.

The best linear unbiased estimator is given by the solution of the following constrained optimization problem

$$\mathbf{\Xi}_k^* = \underset{\mathbf{\Xi}}{\operatorname{argmin}} \sum_{l=1}^{L} \operatorname{Tr} \left(\mathbf{\Xi}^l \mathbf{C}_k^{(l)} \mathbf{\Xi}^{lT} \right),$$

$$\text{s.t.} \quad \sum_{l=1}^{L} \mathbf{\Xi}_k^{l*} = \mathbf{I} \tag{14}$$

where $\mathbf{C}_k^{(l)}$ is the state covariance matrix of the l-th estimator at time k. The method of Lagrange multipliers yields the solution [29]:

$$\mathbf{\Xi}_k^{l*} = \left[\sum_{m=1}^{L} \left(\mathbf{C}_k^{(m)} \right)^{-1} \right]^{-1} \left(\mathbf{C}_k^{(l)} \right)^{-1} \tag{15}$$

Substituting this expression into (13), the optimal linear MMSE (L-MMSE) fusion rule is finally given by

$$\widehat{\mathbf{x}}_k^{(\text{L}-\text{MMSE})} = \left[\sum_{l=1}^{L} \left(\mathbf{C}_k^{(l)} \right)^{-1} \right]^{-1} \sum_{l=1}^{L} \left(\mathbf{C}_k^{(l)} \right)^{-1} \widehat{\mathbf{x}}_k^l \tag{16}$$

regardless of the approach used to derive the partial estimators. Note that, soft fusion is more complex than state overlapping as it requires $L + 1$ matrix inversions of size $D \times D$.

The performance of soft fusion can be improved by overwriting the state vector of each partial estimator by the final estimate (16). In other words, the final estimate of the l-th Kalman filter is

$$\widehat{\mathbf{x}}_k^l = \widehat{\mathbf{x}}_k^{(\text{L}-\text{MMSE})}, \quad l = 1, \dots, L \tag{17}$$

3) Hybrid fusion: Hybrid fusion combines the hard and soft fusion methods in order to take advantage of both. In hybrid fusion, just as in hard fusion, we only consider the partial estimates from those cells where objects reside, but unlike in hard fusion we combine them linearly as

$$\widehat{\mathbf{x}}_k^{(\mathrm{L-MMSE})} = \left[\sum_{m=1}^M \left(\boldsymbol{C}_k^{(l_m)} \right)^{-1} \right]^{-1} \sum_{m=1}^M \left(\boldsymbol{C}_k^{(l_m)} \right)^{-1} \widehat{\mathbf{x}}_k^{l_m} \tag{18}$$

where $\mathbf{C}_k^{(l_m)} = \mathbf{C}_k^{(i)}$ if object m is located in the cell i at time k. Depending on whether the final estimate is going to overwrite the partial estimates, we have two versions of this fusion method. Here we consider only the hybrid method with overwriting because it performs better than the non-overwriting one.

The overwriting procedure and the idea of using multiple local filters instead of a single global one also helps to reduce the probability of divergence. Namely, when a single Kalman filter is in charge of an entire area and that filter diverges, there is no chance of recovery. In contrast, with more than one filter, each will converge or diverge independently from the others. If one filter starts to diverge, the values from the other filters may help to stop divergence by overwriting. Also, since each filter only estimates the location of close objects, the probability of divergence is lower. Together, these facts help to improve the divergence rate.

A. Practical constraints

So far, we have assumed that the exchange of information between the FCs happens instantaneously. In practice, however, there may be a delay that is not negligible compared to the collection interval, and proper adjustments need to be made to accommodate it. Specifically, let T_c denote the collection interval (which satisfies the constraints discussed in Sec. III-B), and let T_d be the delay involved in the information exchange and processing. Upon collecting the sensors' packets over T_c, each FC now makes its local estimate, but delays it until the feedback is received from the neighbors. At this point (after a delay of T_d), it performs fusion. The process then repeats. The location estimates produced by the system now reflect the actual state T_d seconds ago, and the system is updated every $T_c + T_d$. Other than that, the operation remains unchanged.

Other approaches to dealing with the delay are possible as well. For a continuous operation without waiting for the feedback, predictions of the neighbors' local estimates (which are outdated by T_d) can be made before fusion takes place.

V. SIMULATION RESULTS

In this section, we evaluate the performance of the proposed methods through numerical simulation. We consider a large geographical area such as the one shown in Fig. 1. The results in this section are obtained by averaging over 1000 independent realizations for each combination of parameters. The system parameters are chosen to reflect an underwater scenario with limited acoustic bandwidth. To illustrate the results, we assume either an exponential signature with $\alpha = 5$ km^{-1} or an actual acoustic path loss [31]; $\sigma_v = 0.1$ m/s, $T = 1$s, $\rho = 0.999$ and $\bar{L}_p = 10$ bits.

Fig. 3 shows the location mean squared error (MSE) as a function of the object density ρ_o for different rate control schemes and fusion methods. Soft fusion with overwriting (SoftOW) clearly outperforms other methods by a significant margin. Hybrid fusion performs better than hard fusion, while soft fusion without overwriting exhibits the highest MSE. The three rate control schemes perform nearly identically, although relative power outperforms the others slightly. Fig. 3(b) shows the same result, this time for the acoustic path loss model with practical spreading [31].

In Fig. 4 the performance of the SoftOW method is compared for two values of $\mathrm{SNR_c}$ as a function of bandwidth and for various ρ_s and rate control schemes. As we can see from the figure, by increasing the amount of bandwidth, MSE reaches the minimum value corresponding to the perfect communication case (i.e. no packet loss).

Fig. 5 shows the location MSE of the exponential rate control scheme as a function of bandwidth. As we see, the difference between the performance of soft fusion with overwriting and non-overwriting can be more than 20dB. This demonstrates how a simple act of overwriting can have such a significant impact on the performance of the fusion methods.

In Fig. 6 we show the location MSE as a function of the node density ρ_s for different rate control schemes and fusion methods at $\mathrm{SNR_c}$ = -10dB. SoftOW performs better than other fusion methods. Packet throughput is illustrated in Fig. 7 as a function of normalized bandwidth for different node densities and rate control schemes.

In Fig. 8 we compare the performance of the proposed zoning method with that of a single (global) Kalman filter covering the entire area. The area in this example encompasses seven sensing cells. The advantages of zoning are clear for high density of sensor nodes. It is worth mentioning that our goal in introducing zoning was scalability and we were ready to sacrifice some performance for it. However, as we see here, zoning can offer an improvement in performance in addition to enabling geographical scalability.
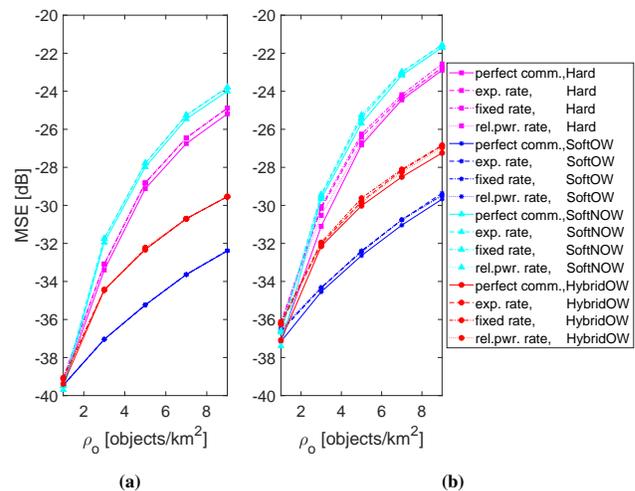

Fig. 3: Location MSE as a function of ρ_o for different rate control schemes and fusion methods. $\rho_s = 28$ nodes/km^2, $p_e = 0.05$, $\mathrm{SNR_c} = -10$dB, and B = 5kHz. (a) exponential path loss with $\alpha = 5$km^{-1} (b) acoustic path loss with $f = 1$kHz, $k = 1.5$, $d_{ref} = 0.1$km.

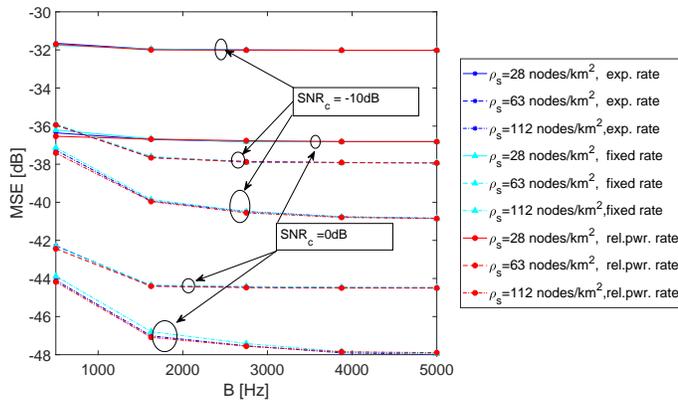This article has been accepted for publication in a future issue of this journal, but has not been fully edited. Content may change prior to final publication. Citation information: DOI 10.1109/JIOT.2020.2988411, IEEE Internet of Things Journal

7

Fig. 4: Location MSE of SoftOW for different ρ_s, two values of $\mathrm{SNR_c}$ and various rate control schemes as a function of bandwidth. $p_e = 0.05$, $\rho_o = 9$ objects/km^2.
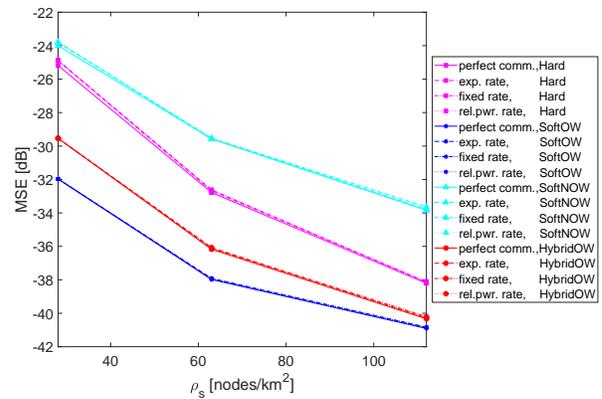

Fig. 6: Location MSE for different rate control schemes and fusion methods as a function of ρ_s at $\mathrm{SNR_c} = -10$dB and B. $p_e = 0.05$, B = 5kHz, $\rho_o = 9$ objects/km^2.
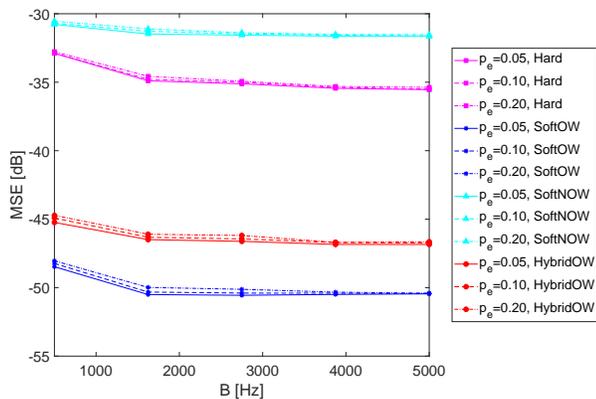

Fig. 5: Location MSE of the exponential rate control scheme for different p_e, various fusion methods as a function of bandwidth. $\mathrm{SNR_c} = 10$dB, $\rho_o = 9$ objects/km^2, $\rho_s = 63$ nodes/km^2, and $p_e = 0.05$.
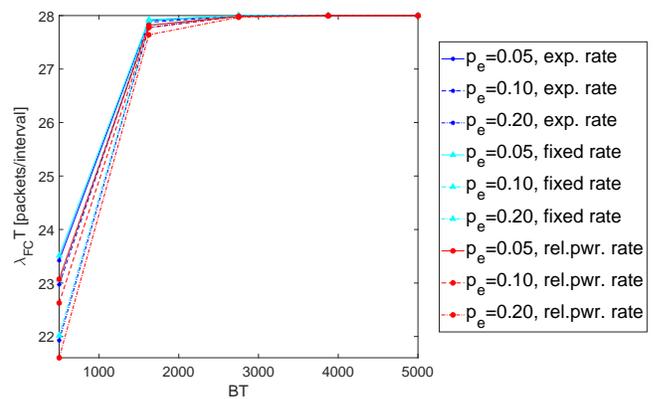

Fig. 7: Packet rate at FC as a function of BT for different p_e and rate control schemes. $\rho_o = 9$ objects/km^2, $\mathrm{SNR_c} = -10$dB, $\rho_s = 28$ nodes/km^2.

The effect of waiting is quantified in Fig. 9. This figure shows the system performance (localization MSE in the delayed estimate) as a function of delay T_d. We note that the effect of delay is not detrimental for a considerable range of the values T_d. Assuming a radio link between the FCs and $T_c = 1$s, $T_d = 5$s or 10s would be well within the range of practical delays.

VI. CONCLUSION

We outlined a method for designing random access sensor network for object tracking, with a focus on scenarios where large area coverage is needed. Our design is based on the idea of zoning, where the entire observation area is divided into design units (DUs), which in turn consist of a number of sensing cells. Independence of the design units is ensured by postulating the isolation rule according to which nodes located in the central cell of a DU sense only the objects within the DU but not outside of it. These sensors report to their local fusion center which runs an extended Kalman filter. The size of the corresponding state vector is chosen so as to accommodate the objects inside the DU. We proposed a systematic approach to determining the cell size, updating interval, transmission rate and other salient system parameters in a way that ensures the

desired performance given a limited amount of bandwidth and imperfect communication links where data packets get lost to communication noise and collisions. Rate control schemes were additionally introduced to improve the bandwidth efficiency of the network, and fusion methods were designed to combine location estimates of individual cells' EKFs in an
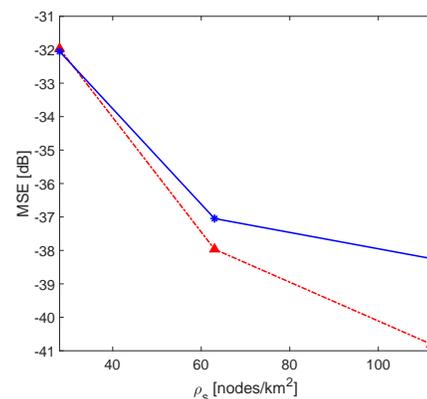

Fig. 8: Performance comparison between zoning and global Kalman filtering for SoftOW as a function of ρ_s. $\rho_o = 9$ objects/km^2, $\mathrm{SNR_c} = -10$dB, $p_e = 0.05$, and B = 5kHz. $*$: global, ▲ : zoning
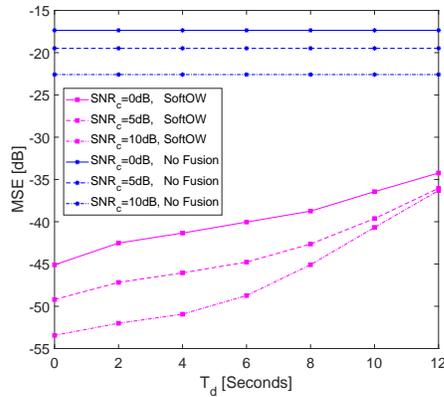
Fig. 9: MSE of SoftOW for various SNR_c's as a function of delay. $\rho_o = 3$ objects/km^2, $T_c = 1s$ and $\alpha = 5$km^{-1}. Perfect communications (no packet loss) is considered. The average speed is 4.7m/s. The MSE of no fusion method is shown as the benchmark.

efficient manner to improve the overall performance, resolve the cell crossing issue, and ensure scalability to an arbitrary coverage area.

The proposed method is fully scalable and applies to an arbitrary coverage area with only a linear increase in complexity and the total power consumed. Computational complexity is determined by the number of objects expected in one DU, while the power consumed in one sensing cell is determined by the size of the cell (power consumed in each additional cell adds linearly). Thus, the algorithm retains the same computational complexity, while the total coverage area can grow without bounds.

Although our numerical examples focused on underwater acoustic communication scenario and exponential path loss models, the methods proposed are not limited to this case and can be applied to terrestrial radio and other systems as well. Future research will focus on finding additional rate adjustment policies, taking into account factors such as the speed of objects, as well as mobile systems, where the sensors' locations can be controlled.

REFERENCES

[1] I. Khan, F. Belqasmi, R. Glitho, N. Crespi, M. Morrow, and P. Polakos, "Wireless sensor network virtualization: A survey," *IEEE Commun. Surveys Tuts*, vol. 18, no. 1, pp. 553–576, 2016.

[2] É. L. Souza, E. F. Nakamura, and R. W. Pazzi, "Target tracking for sensor networks: A survey," *ACM Computing Surveys (CSUR)*, vol. 49, no. 2, p. 30, 2016.

[3] J. Heidemann, M. Stojanovic, and M. Zorzi, "Underwater sensor networks: applications, advances and challenges," *Phil. Trans. R. Soc. A*, vol. 370, no. 1958, pp. 158–175, 2012.

[4] M. Stojanovic and J. Preisig, "Underwater acoustic communication channels: Propagation models and statistical characterization," *IEEE communications magazine*, vol. 47, no. 1, pp. 84–89, 2009.

[5] A. C. Singer, J. K. Nelson, and S. S. Kozat, "Signal processing for underwater acoustic communications," *IEEE Communications Magazine*, vol. 47, no. 1, pp. 90–96, 2009.

[6] R. W. Coutinho, A. Boukerche, L. F. Vieira, and A. A. Loureiro, "Geographic and opportunistic routing for underwater sensor networks," *IEEE Transactions on Computers*, vol. 65, no. 2, pp. 548–561, 2015.

[7] U. Mitra, S. Choudhary, F. Hover, R. Hummel, N. Kumar, S. Naryanan, M. Stojanovic, and G. Sukhatme, "Structured sparse methods for active ocean observation systems with communication constraints," *IEEE Commun. Mag.*, vol. 53, no. 11, pp. 88–96, 2015.

[8] J. Luo, Y. Han, and L. Fan, "Underwater acoustic target tracking: A review," *Sensors*, vol. 18, no. 1, p. 112, 2018.

[9] J. Kumari, P. Kumar, and S. K. Singh, "Localization in three-dimensional wireless sensor networks: a survey," *J. Supercomput.*, pp. 1–44, 2019.

[10] D. Dardari, P. Closas, and P. M. Djurić, "Indoor tracking: Theory, methods, and technologies," *IEEE Transactions on Vehicular Technology*, vol. 64, no. 4, pp. 1263–1278, 2015.

[11] S. Biswas, R. Das, and P. Chatterjee, "Energy-efficient connected target coverage in multi-hop wireless sensor networks," in *Industry interactive innovations in science, engineering and technology*. Springer, 2018, pp. 411–421.

[12] A. Tripathi, H. P. Gupta, T. Dutta, D. Kumar, S. Jit, and K. Shukla, "A target tracking system using directional nodes in wireless sensor networks," *IEEE Systems Journal*, vol. 13, no. 2, pp. 1618–1627, 2018.

[13] L. Gao, G. Battistelli, L. Chisci, and P. Wei, "Distributed joint sensor registration and target tracking via sensor network," *Information Fusion*, vol. 46, pp. 218–230, 2019.

[14] H. Zhang, X. Zhou, Z. Wang, H. Yan, and J. Sun, "Adaptive consensus-based distributed target tracking with dynamic cluster in sensor networks," *IEEE transactions on cybernetics*, vol. 49, no. 5, pp. 1580–1591, 2018.

[15] M. Anvaripour, M. Saif, and M. Ahmadi, "A novel approach to reliable sensor selection and target tracking in sensor networks," *IEEE Transactions on Industrial Informatics*, 10 May 2019, doi=10.1109/TII.2019.2916091.

[16] W.-P. Chen, J. C. Hou, and L. Sha, "Dynamic clustering for acoustic target tracking in wireless sensor networks," *IEEE Trans. Mobile Comput.*, vol. 3, no. 3, pp. 258–271, 2004.

[17] H. Ramezani, F. Fazel, M. Stojanovic, and G. Leus, "Collision tolerant and collision free packet scheduling for underwater acoustic localization," *IEEE Trans. Wireless Commun.*, vol. 14, no. 5, pp. 2584–2595, 2015.

[18] A. L. Rodriguez and M. Stojanovic, "Adaptive object tracking in a sensor network," in *OCEANS 2015-Genova*. IEEE, 2015, pp. 1–5.

[19] M. Alimadadi, M. Stojanovic, and P. Closas, "Object tracking using modified lossy extended Kalman filter," in *Proc. Int. Conf. Underwater Netw. & Syst.* ACM, 2017, p. 7.

[20] B. Sinopoli, L. Schenato, M. Franceschetti, K. Poolla, M. I. Jordan, and S. S. Sastry, "Kalman filtering with intermittent observations," *IEEE Trans. Autom. Control*, vol. 49, no. 9, pp. 1453–1464, 2004.

[21] A. Dana, V. Gupta, J. Hespanha, B. Hassibi, and R. Murray, "Estimation over communication networks: Performance bounds and achievability results," in *2007 American Control Conference*. IEEE, 2007, pp. 3450–3455.

[22] D. E. Quevedo, A. Ahlen, and K. H. Johansson, "State estimation over sensor networks with correlated wireless fading channels," *IEEE Transactions on Automatic Control*, vol. 58, no. 3, pp. 581–593, 2012.

[23] K. You, N. Xiao, and L. Xie, "Kalman filtering with scheduled measurements," in *Analysis and Design of Networked Control Systems*. Springer, 2015, pp. 269–291.

[24] D. E. Marelli, T. Sui, E. R. Rohr, and M. Fu, "Stability of Kalman filtering with a random measurement equation: Application to sensor scheduling with intermittent observations," *Automatica*, vol. 99, pp. 390–402, 2019.

[25] H. S. Karimi and B. Natarajan, "Kalman filtered compressive sensing with intermittent observations," *Signal Processing*, vol. 163, pp. 49–58, 2019.

[26] G. Wang, N. Li, and Y. Zhang, "Diffusion nonlinear Kalman filter with intermittent observations," *Proceedings of the Institution of Mechanical Engineers, Part G: Journal of Aerospace Engineering*, vol. 232, no. 15, pp. 2775–2783, 2018.

[27] I. Arasaratnam and S. Haykin, "Cubature Kalman filters," *IEEE Transactions on automatic control*, vol. 54, no. 6, pp. 1254–1269, 2009.

[28] F. Fazel, M. Fazel, and M. Stojanovic, "Random access compressed sensing over fading and noisy communication channels," *IEEE Trans. Wireless Commun.*, vol. 12, no. 5, pp. 2114–2125, 2013.

[29] D. Luengo, L. Martino, V. Elvira, and M. Bugallo, "Efficient linear fusion of partial estimators," *Digital Signal Processing*, vol. 78, pp. 265–283, 2018.

[30] M. Alimadadi, M. Stojanovic, and P. Closas, "Object tracking in random access sensor networks: Extended Kalman filtering with state overlapping," in *IEEE INFOCOM 2019-IEEE Conference on Computer Communications Workshops (INFOCOM WKSHPS)*. IEEE, 2019, pp. 927–932.

[31] P. Qarabaqi and M. Stojanovic, "Statistical characterization and computationally efficient modeling of a class of underwater acoustic communication channels," *IEEE Journal of Oceanic Engineering*, vol. 38, no. 4, pp. 701–717, 2013.